ACCELERATED FIRST PASS CARDIAC PERFUSION MRI USING IMPROVED $k-t$ SLR

Sajan G Lingala[*]*, Yue Hu*[*]*, Edward Dibella*[†] *and Mathews Jacob*[*]

[*]Department of Biomedical Engineering, University of Rochester, NY, USA
[†]Department of Radiology, University of Utah, UT, USA

ABSTRACT

Routinely trade-offs between the spatio-temporal resolution, volume coverage and SNR are done in first pass cardiac perfusion MRI due to the restricted imaging acquisition window (usually of the order of 300 to 400 msec per heart beat). In this paper, we demonstrate the use a low rank and sparse reconstruction scheme ($k-t$ SLR) in obtaining highly accelerated first pass perfusion MR images and hence aim to reduce the above mentioned trade-offs. We introduce non-convex spectral norms and use a spatio-temporal total variation norm in recovering the dynamic signal matrix. We introduce an augmented Lagrangian optimization scheme in the context of matrix recovery to speed up the convergence of the algorithm. Extensive validations on in-vivo data are done to demonstrate the performance improvement of the proposed frame work.

1. INTRODUCTION

First pass cardiac perfusion magnetic resonance imaging (MRI) has been gaining significant clinical importance due to its potential to assess coronary artery disease. Perfusion imaging track the dynamic variations of a contrast agent as it traverses through different regions of the heart. The acquisition window is typically restricted to the diastolic phase to minimize the motion interference due to cardiac pumping. The need for acceleration to acquire images within this limited imaging window is of prime importance to reduce the compromises between the spatial resolution, temporal resolution, SNR and slice coverage.

Several accelerated $k-t$ reconstruction schemes that rely on the structure or sparsity in $x-f$ space have been proposed [1, 2]. These schemes are originally designed for breath held applications and for representing signals which are approximately periodic such as in cardiac cine imaging. The $x-f$ space's structure and sparsity are disturbed due to the bolus passage and motion (usually present in long breath hold or free breathing studies) limiting the application of these methods to perfusion imaging [3]. Recently, the interest has been on Karhunen Loeve Transform (KLT) / Principal Component Analysis (PCA) schemes that exploit the inherent redundancy of dynamic data without explicitly modeling the temporal variations. These schemes estimate the temporal bases from the data itself and hence are guaranteed to provide a compact representation, making it an attractive tool for accelerated first pass perfusion imaging. However, the practical realization of these schemes have trade offs between suppression of spatial aliasing and accurate temporal modeling [4]. We recently proposed a regularized frame work with low rank and sparsity penalties that breaks this trade off and recovers the temporal bases and spatial weights directly from the measured data [5]. In this paper, we further improve our frame work by introducing the following modifications and demonstrate its feasibility in acquiring highly accelerated first pass perfusion images:

- Use of non convex spectral priors: Motivated by improved performance of l_p penalties compared to l_1 in compressed sensing, we propose to use the non convex Schatten p-norm matrix penalty. Specifically, this term weights the small singular values/vectors, which often correspond to aliasing artifacts, more heavily than others, thus suppressing them in the reconstructions; this provides reconstructions with better fidelity for a specified acceleration factor.
- Use of spatio-temporal total variation sparsity priors: Our implementation in [5] was for ungated real time cardiac MRI, where we used the sparsity penalty in the $x-f$ space. In this work, we propose to exploit the sparsity of the gradients of the data in the spatio-temporal directions by using the total variation (TV) norm.
- Use of augmented Lagrangian optimization solver: The convergence of the continuation optimization scheme used in [5] was sensitive to the specific choice of the continuation parameters. In this work, we address this by introducing an augmented Lagrangian (AL) solver that considerably improves the convergence properties.

2. IMPROVED $k-t$ SLR

In first pass perfusion imaging, different anatomical regions of the heart (such as the voxels within the right ventricle or the myocardium) share similar temporal characteristics. This

This work is supported by NSF award CCF-0844812 and in part by NIH R01EB006155.

property allows us to assume the voxel time series to lie in a low-dimensional space. Specifically the dynamic signal $\gamma(\mathbf{x}, t)$ can be represented as a matrix that has linearly dependent rows i.e, low rank (see equations 1 to 4 in [5]; here, we use the same notations).

We pose the recovery of both the temporal bases and spatial weights as a regularized matrix recovery problem with low rank and sparsity penalties. Specifically, we recover $\mathbf{\Gamma}$ by using a non convex spectral norm and exploit the sparsity of the row and column spaces of $\mathbf{\Gamma}$ by using the total variation norm. We formulate the problem as:

$$\mathbf{\Gamma}^* = \arg\min_{\mathbf{\Gamma}} \|\mathcal{A}(\mathbf{\Gamma}) - \mathbf{y}\|^2 + \lambda_1\, \varphi(\mathbf{\Gamma}) + \lambda_2\, \psi(\mathbf{\Gamma}), \quad (1)$$

The non convex spectral norm $\varphi(\mathbf{\Gamma}) = (\|\mathbf{\Gamma}\|_p)^p = \sum_{i=1}^{\min\{m,n\}} \sigma_i^p$ penalizes the small singular values often associated with artifacts more strongly than the convex nuclear norm ($p = 1$). The use of the TV prior restricts the search space to smaller class of matrices by penalizing irregular solutions whose left and right singular vectors are not sparse; this property can allow for efficient recovery of $\mathbf{\Gamma}$ from very few measurements. The TV norm based on the gradient of the entire volume is specified by

$$\psi(\mathbf{\Gamma}) = \left\| \sqrt{\sum_{i=0}^{2} |\mathbf{\Phi}_i^* \mathbf{\Gamma} \mathbf{\Psi}_i|^2} \right\|_{\ell_1} \quad (2)$$

where $\mathbf{\Phi}_0 = \mathbf{D}_x; \mathbf{\Psi}_0 = \mathbf{I}$, $\mathbf{\Phi}_1 = \mathbf{D}_y; \mathbf{\Psi}_1 = \mathbf{I}$, and $\mathbf{\Phi}_2 = \mathbf{I}; \mathbf{\Psi}_2 = \mathbf{D}_t$; $\mathbf{D}_x$, $\mathbf{D}_y$ and $\mathbf{D}_t$ are the finite difference matrices along x, y, and t respectively.

2.1. The augmented Lagrangian (AL) solver

We first convert (2) to an equivalent constrained problem, which is easier to solve, by introducing two auxiliary variables $\mathbf{S}$ and $\mathbf{T}$

$$\mathbf{\Gamma}^* = \arg\min_{\mathbf{\Gamma},\mathbf{S},\mathbf{T}} \|\mathcal{A}(\mathbf{\Gamma}) - \mathbf{b}\|^2 + \lambda_1 (\|\mathbf{S}\|_p)^p + \lambda_2 \left\| \sqrt{\sum_{i=0}^{2} \|\mathbf{T}_i\|^2} \right\|_{\ell_1}$$
$$\text{s.t. } \mathbf{\Gamma} = \mathbf{S};\ \ \mathbf{T}_i = \mathbf{\Phi}_i^* \mathbf{\Gamma} \mathbf{\Psi}_i;\ i = 0, 1, 2 \quad (3)$$

We now solve the above constrained problem using the AL method (also termed as the multiplier method) [6, 7]. Specifically, we consider the following modified cost function:

$$\mathcal{D} = \|\mathcal{A}(\mathbf{\Gamma}) - \mathbf{b}\|^2 + \lambda_1 (\|\mathbf{S}\|_p)^p + \lambda_2 \left\| \sqrt{\sum_{i=0}^{2} \|\mathbf{T}_i\|^2} \right\|_{\ell_1} \quad (4)$$
$$+\beta_1 \|\mathbf{\Gamma} - \mathbf{S}\|^2/2 + \beta_2 \sum_{i=0}^{2} \|\mathbf{\Phi}_i^* \mathbf{\Gamma} \mathbf{\Psi}_i - \mathbf{T}_i\|^2/2 +$$
$$\beta_1 \langle \mathbf{X}, \mathbf{\Gamma} - \mathbf{S} \rangle + \beta_2 \sum_{i=0}^{2} \langle \mathbf{Y}_i, \mathbf{\Phi}_i \mathbf{\Gamma} \mathbf{\Psi}_i - \mathbf{T}_i \rangle$$

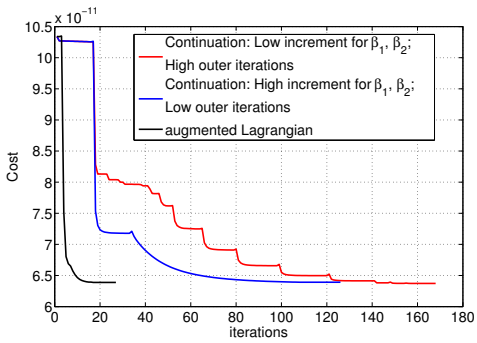

Fig. 1: Convergence analysis: The continuation scheme is highly dependent on the increments of the continuation parameters. Here we demonstrate two specific cases. The augmented Lagrangian method converges in 25 iterations, while the best continuation (the fastest) scheme takes 120 iterations. The computational complexity for these 3 schemes on the GPU were 1.8 min (augmented Lagrangian), 8.2 min (Fast continuation) and 9.5 min (Slow continuation).

where $\mathbf{X}$ and $\mathbf{Y}_i$ are matrices of Lagrange multipliers and the inner product of two matrices is specified by $\langle \mathbf{A}, \mathbf{B} \rangle = \text{trace}(\mathbf{A}^T \mathbf{B})$. Penalty methods (without the Lagrange multiplier terms; i.e, the third line of (4)) with continuation alternately minimize the variable of interest and the auxiliary variables while slowly taking the values of β_1 and β_2 to high values to enforce the constraints in (3). However, when β_1, β_2 grow large, the problem gets ill-conditioned leading to more number of conjugate gradient steps and hence slow convergence. The AL method has been shown to ensure fast convergence. Moreover it does not require β_1 and β_2 to tend to high values [6, 7]. In contrast to the three step minimization scheme used in [5], we propose to use a five step AL scheme which requires to additionally update $\mathbf{X}$ and $\mathbf{Y}_i$:

$$\mathbf{\Gamma}_{n+1} = \arg\min_{\mathbf{\Gamma}} \|\mathcal{A}(\mathbf{\Gamma}) - \mathbf{b}\|^2 + \frac{\beta_1}{2} \|\mathbf{\Gamma} - (\mathbf{S}_n - \mathbf{X}_n)\|^2 +$$
$$\frac{\beta_2}{2} \sum_{i=0}^{2} \|\mathbf{\Phi}_i^* \mathbf{\Gamma} \mathbf{\Psi}_i - (\mathbf{T}_{i,n} - \mathbf{Y}_{i,n})\|^2 \quad (5)$$

$$\mathbf{S}_{n+1} = \arg\min_{\mathbf{S}} \|(\mathbf{\Gamma}_{n+1} + \mathbf{X}_n) - \mathbf{S}\|^2 + \lambda_1/2\beta_1 (\|\mathbf{S}\|_p)^p \quad (6)$$

$$\mathbf{T}_{i,n+1} = \arg\min_{\{\mathbf{T}_i\}} \sum_{i=0}^{2} \|\underbrace{\mathbf{\Phi}_i^* \mathbf{\Gamma}_{n+1} \mathbf{\Psi}_i + \mathbf{Y}_{i,n}}_{\mathbf{P}_i} - \mathbf{T}_i\|^2 +$$
$$\lambda_2/2\beta_2 \left\| \sqrt{\sum_{i=0}^{q-1} \|\mathbf{T}_i\|^2} \right\|_{\ell_1};\ i = 0, 1, 2 \quad (7)$$

$$\mathbf{X}_{n+1} = \mathbf{X}_n + (\mathbf{\Gamma}_{n+1} - \mathbf{S}_{n+1}) \quad (8)$$

$$\mathbf{Y}_{i,n+1} = \mathbf{Y}_{i,n} + (\mathbf{\Phi}_i^* \mathbf{\Gamma}_{n+1} \mathbf{\Psi}_i - \mathbf{T}_{i,n+1});\ i = 0, 1, 2. \quad (9)$$

We propose to solve the quadratic minimization problem, specified by (5), using a few iterations of the conjugate gradient (CG) algorithm. Since we do not have to use very high values of β_1 and β_2, the CG scheme requires few number of steps (around 3-4) in most cases. (6) is solved as the singular value shrinkage below (10):

$$\mathbf{S}_{n+1} = \sum_{i=0}^{\max(m,n)} \left(\sigma_i - \lambda_1\, \sigma_i^{p-1}/\beta\right)_+ \mathbf{u}_i \mathbf{v}_i^*, \quad (10)$$

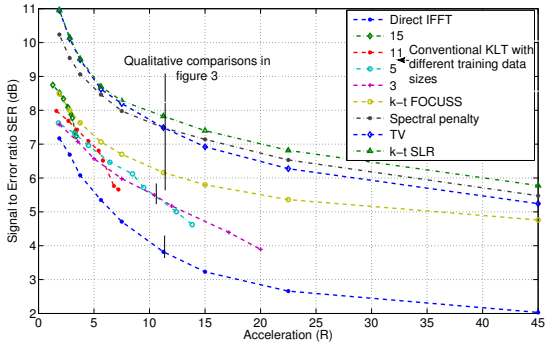

Fig. 2: SER v/s acceleration for different schemes: k-t SLR out performs most of the methods consistently at a range of accelerations. The difference between k-t SLR and TV increases at accelerations greater than 5. Visual comparisons at $R \approx 11$ are shown in figure 3.

where $()_+$ is a shrinkage operator that returns the input when its greater than zero else returns zero. The solution of (7) involves the joint processing of all the terms $\mathbf{P}_i; i = 0, 1, 2$, such that the magnitude $\sum_{i=0}^{2} \|\mathbf{P}_i\|^2$, is shrunk:

$$\mathbf{T}_{i,n+1} = \frac{\mathbf{P}_i}{\sum_{i=0}^{2} \|\mathbf{P}_i\|^2} \cdot \left(\sum_{i=0}^{2} \|\mathbf{P}_i\|^2 - \frac{\lambda_2}{\beta_2} \right)_+ \qquad (11)$$

where $\mathbf{P}_i = \mathbf{\Phi}_i^* \mathbf{\Gamma}_{n+1} \mathbf{\Psi}_i + \mathbf{Y}_{i,n}$. This approach is termed as multidimensional shrinkage of $\{\mathbf{P}_i, i = 0, 1, 2\}$ [8]. The steps (8) and (9) are the updates of the Lagrange multipliers $\mathbf{X}$ and $\mathbf{Y}_i; i = 0, 1, 2$ and are standard. Using continuation in AL frame work is usually recommended to further increase the convergence. Hence, we initialize $\beta_1 > 0$ and $\beta_2 > 0$ as small values and gradually increase them. Thanks to the fast convergence of the AL scheme, we do not require carefully designed continuation strategies or increase the penalty weights to very high values.

3. RESULTS

We show the performance evaluation on an in-vivo first pass perfusion data set acquired on a 3T Siemens scanner at the University of Utah in accordance with the institute's review board. The data was acquired on a Cartesian grid with 90 phase encodes and a temporal resolution of one heart beat. 190 readouts and 70 time frames were obtained. The subject was not able to hold his breath for the entire imaging duration and the data contained residual breathing motion. We implemented the entire algorithm, described by (5)-(9), in MATLAB using Jacket on a Linux workstation with eight cores and a NVDIA Tesla graphical processing unit. The computationally expensive component of the algorithm is the singular value decomposition required for (7). The size of the $\mathbf{\Gamma}$ matrix was 17100 x 70. We implemented the SVD as the eigen decomposition of $\mathbf{\Gamma}^H \mathbf{\Gamma}$. The left singular vectors are obtained using a simple least squares scheme. The eigen decomposition of a 70x70 matrix takes less than 0.1 seconds. The entire algorithm is computationally efficient and usually took 90 to 150 seconds of execution time.

3.1. Convergence of the algorithm

In figure 1, we describe the convergence of the proposed scheme using the continuation scheme and AL method. We observe a significant speed up (four to five fold) in our application by using the AL method. It is seen from figure 1 that the AL scheme converges very fast while the continuation schemes depend on the choice of β_1 and β_2 increments.

3.2. Comparison with different methods

We compare our $k-t$ SLR method against the following state of the art acceleration schemes at a range of accelerations (R); (R is defined as the ratio of the actual number of acquired phase encodes to the number of encodes used in the reconstruction):

- Conventional two step KLT schemes [4] that rely on a training data set with low spatial but high temporal resolution to estimate the temporal bases and uses it to estimate the spatial weights from sparse $k-t$ samples. We consider a range of training data sizes.
- A model based $x-f$ scheme: We consider $k-t$ FOCUSS [9] which has shown to be an improvised version of related methods like $k-t$ BLAST and UNFOLD.
- Regularized schemes that rely only on using (a) the spectral penalty ($\lambda_2 = 0$) or (b) the TV penalty ($\lambda_1 = 0$)

The conventional KLT scheme uses Cartesian trajectories. All the other schemes uses an equi-angled radial trajectory in each frame which is rotated by a random angle across frames to achieve incoherent sampling. All the schemes were initialized with the zero filled IFFT reconstructions and were iterated until convergence. We use the signal to error ratio as measure to provide a quantitative index of the performance.

$$\text{SER} = -10 \log_{10} \frac{\|\mathbf{\Gamma}_{\text{rec}} - \mathbf{\Gamma}_{\text{fullysampled}}\|_F^2}{\|\mathbf{\Gamma}_{\text{fullysampled}}\|_F^2}, \qquad (12)$$

where $\|\cdot\|_F$ is the Frobenius norm.

It is seen from figure 2 that $k-t$ SLR out performs its closest competitors by 1-2 dB at most accelerations. The performance of TV based regularizer is close to $k-t$ SLR at low accelerations $(R < 5)$. However at higher accelerations, it results in significant spatial smoothing and loss of details as demonstrated in figure 2.

In figure 3, we show visual comparisons at a high acceleration $(R \approx 11)$. We observe compromise in the spatial quality at the expense of accurate temporal modeling in the KLT scheme, motion blur in $k-t$ FOCUSS due to the failure of meeting sparsity constraints in the $x-f$ space, residual streak artifacts and over smoothing respectively in using only the spectral and the TV penalties which are all minimized in $k-t$ SLR.

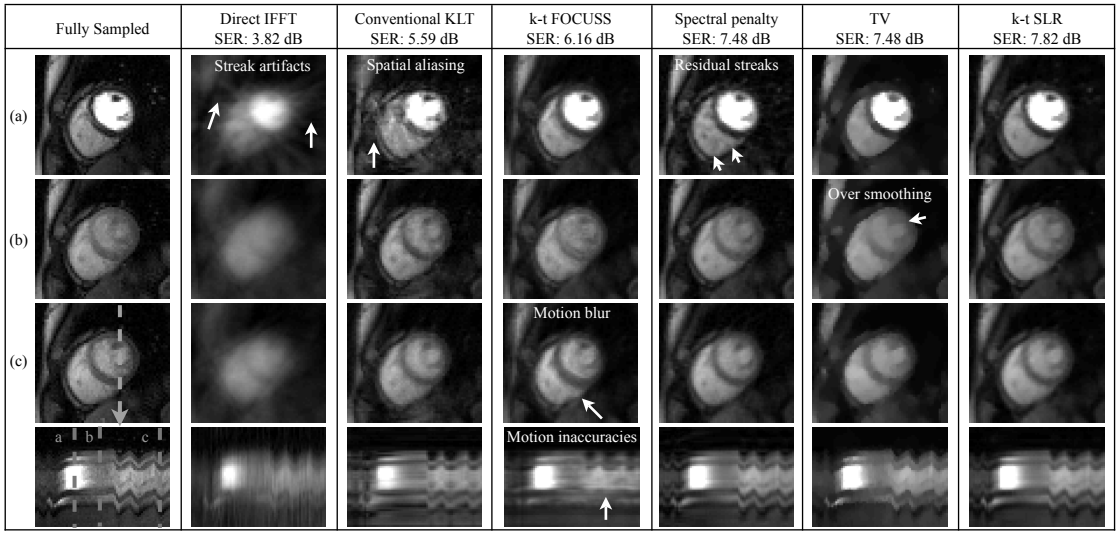

Fig. 3: Comparisons on in-vivo data at 11 fold acceleration: The first column of the left shows the fully sampled data, while columns 2 to 7 show the reconstructions using direct IFFT, best of the conventional two-step KLT schemes, $k-t$ FOCUSS method, Spectral penalty, TV and the $k-t$ SLR scheme. We choose R = 11.2 for all the methods except the two-step KLT, which is at an acceleration of R = 10.2. The KLT scheme that had the best SER was picked (see Fig. 2). The top row shows the reconstructed frames at peak LV uptake, the second row shows peak myocardial uptake, the third row shows post contrast during breathing and the bottom row shows the image time series ($x-t$ plot) corresponding to the dotted arrow in (c). The temporal instances of the spatial frames shown in the top three rows are marked in the image time series of the fully sampled data. We observe that the reconstructions with the two-step KLT scheme exhibit significant spatial aliasing, indicated by arrow. The $k-t$ FOCUSS reconstructions exhibit temporal inaccuracies, which can be appreciated from the time series images in the bottom row. The spectral penalty has noisy artifacts as shown by the arrows in the corresponding inset of (a). Over smoothing and blurring of important details such as the borders of the heart and the papillary muscles are seen in the TV reconstructions. In contrast, the $k-t$ SLR scheme gives efficient reconstructions with minimal blurring.

4. CONCLUSIONS

We demonstrated the utility of k-t SLR in acquiring highly accelerated first pass perfusion images. The method of $k-t$ SLR was improved to cater to the requirements of perfusion imaging, where we used non convex spectral priors and spatio-temporal TV norms. The use of the augmented Lagrangian optimization solver provided a significant (4 to 5 fold) improvement over continuation schemes in the computational speed of the algorithm. Our results demonstrate efficient reconstructions with $k-t$ SLR at accelerations as high as 11 fold, while most of the existing schemes suffer from artifacts. These improvements could be practically used to obtain high spatio-temporal resolutions and volume coverage in first pass perfusion imaging.

5. ACKNOWLEDGEMENT

We thank Dr. Sathish Ramani of University of Michigan for his insightful discussions and comments in improving the optimization algorithm.

6. REFERENCES

[1] Z. Liang, H. Jiang, C. Hess, and P. Lauterbur, "Dynamic imaging by model estimation," *International Journal of Imaging Systems and Technology*, vol. 8, no. 6, pp. 551–557, 1997.

[2] J. Tsao, P. Boesiger, and K. Pruessmann, "kt BLAST and kt SENSE: dynamic MRI with high frame rate exploiting spatiotemporal correlations," *Magnetic Resonance in Medicine*, vol. 50, no. 5, pp. 1031–1042, 2003.

[3] G. Adluru, S. Awate, T. Tasdizen, R. Whitaker, and E. DiBella, "Temporally constrained reconstruction of dynamic cardiac perfusion MRI," *Magnetic Resonance in Medicine*, vol. 57, no. 6, pp. 1027–1036, 2007.

[4] C. Brinegar, Y. Wu, L. Foley, T. Hitchens, Q. Ye, C. Ho, and Z. Liang, "Real-time cardiac MRI without triggering, gating, or breath holding," in *International Conference of the IEEE Engineering in Medicine and Biology Society, 2008. EMBS 2008*, 2008, pp. 3381–3384.

[5] S. Goud, Y. Hu, and M. Jacob, "Real-time cardiac MRI using low-rank and sparsity penalties," in *Proceedings of the ISBI, 2010*.

[6] D. Bertsekas, "Multiplier methods: a survey," *Automatica*, vol. 12, no. 2, pp. 133–145, 1976.

[7] M. Afonso, J. Bioucas-Dias, and M. Figueiredo, "Fast image recovery using variable splitting and constrained optimization," *Image Processing, IEEE Transactions on*, vol. 19, no. 9, pp. 2345–2356, 2010.

[8] J. Yang and Y. Zhang, "Alternating direction algorithms for l1-problems in compressive sensing," *preprint*, 2009.

[9] H. Jung, J. Park, J. Yoo, and J. C. Ye, "Radial k-t FOCUSS for high-resolution cardiac cine MRI," *Magnetic Resonance in Medicine*, Oct 2009.